

*P. Ottosson¹, E.-L. Westman¹, I. Nygren², T. Pettersson³, F. Niklasson⁴, L.-E. Brattström⁴

¹RISE Research Institutes of Sweden, Unit Component Manufacturing, Box 104, SE-431 22 BoråsPhone: +46 10 228 47 10, E-mail: peter.ottosson@ri.se

²Quintus Technologies, Quintusvägen 2, SE-721 36 Västerås

³Permanova LaserTool in Blekinge, Vällaregatan 30, 293 38 Olofström

⁴GKN Aerospace Engine Systems Sweden, Dept.9655 - TK3, SE-461 81 Trollhättan

Abstract

In this work, a forming procedure for a geometry of interest to the aero engine industry was studied and proposed. The development work was performed according to the principle "first time right" in which careful material model calibration and FE-analyses of the anisotropic superalloy 718 and the Flexform™ procedure resulted in high correlation between predicted and measured responses. The influence from different process parameters such as friction coefficient, material property variations and blank design to the material thinning, spring back behavior and shape accuracy was investigated thorough a parameter study. By forming a suitable geometry from the metal sheet and subsequently machine to the desired component shape, the work was able to demonstrate the sustainability potential. A simplified life cycle analysis indicates that a decrease in energy consumption of 50% was reached, compared to the production method currently applied.

Keywords: Forming process, material modelling, FE-modelling, parameter study, experimental validation

1. General Introduction

The aero engine industry in Sweden continuously strive to develop abilities, processes and products for lightweight solutions that in a fast pace contribute to a sustainable society. GKN Aerospace Engine Systems Sweden and sub-suppliers explore and demonstrate new variants of manufacturing process chains for products that will power fossil free transportation in Sweden and abroad. In this study, a manufacturing procedure for a load carrying aero engine component in alloy 718 was evaluated, including FlexformTM (Flexform) and mechanical cutting. The project had a target to considerably reduce material, time and energy consumption by at least 50% each. The virtual die and process design for the Flexform procedure involved FE-modeling, anisotropic material model calibration and parameter studies to identify best choice in blank design and process parameters with respect to minimal spring back. Predicted responses were compared with measured results from Flexform tests. Alloy 718 in the annealed condition possess anisotropic properties and is one of the most frequently used alloys in aircraft engines due to its high strength, good ductility, and corrosion resistance at elevated temperatures [1-4].

Existing multi-step manufacturing procedures of representative aero engine components are to a high extent based on a forging processes following machining to reach final geometry. This implies high levels of energy, material, and time consumption to a relatively high cost. The Flexforming process is a low-cost sheet metal hydroform technology, ideally suited for low volume production. Flexform use only one single tool half and a flexible rubber diaphragm, backed up by high-pressure hydraulic oil and are a process that often result in a reduced amount of spring back upon unloading compared to other forming procedures [6-9]. In this project the Flexform method is applied to form a geometry that requires minimal machining to directly obtain the final part tolerances for production. The deep drawing Flexform method imply that the metal blank is placed on a fixed draw ring whereas the punch is movable as presented in Figure 1.

Flexform, also called fluid cell forming, is a low-cost sheet metal forming process designed for both prototyping and lower volume parts production. The Flexform technique has shown to contribute to

an efficiency increase in low-volume production [5]. The method implies high pressure which yields possibilities to eliminate process steps and improve fabrication productivity. The Flexform method requires only one tool half and also a draw ring, placed on the moving press table. See Figure 1. The blank material is placed on the tool half before the press table returns to its position in the press. The forming process takes place by pressurizing the rubber membrane with a liquid, usually oil, whereby the sheet blank is formed to the desired geometry.

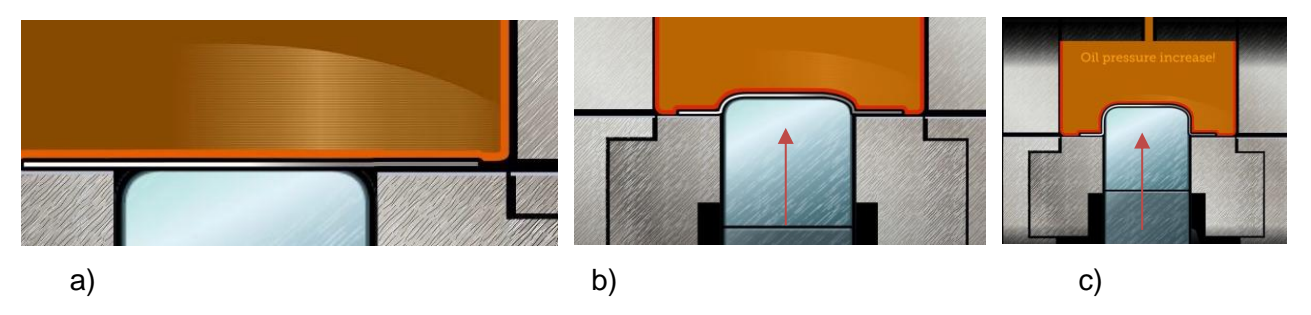


Figure 1 Illustration of the principle of the Flexform process and movements of tool components. a) The flat blank material placed on the draw ring, b) pressurized oil above the membrane and the punch moving upwards in the direction of the arrow, c) further punch travel upwards causing an increased oil pressure restricting the blank and the draw-in during the forming procedure.

2. Modelling the Flexform process

The material studied in this work is alloy 718 with a sheet thickness of 10.0 mm. The material is a precipitation-hardening nickel-chromium alloy containing significant amounts of iron, niobium, and molybdenum with minor amounts of aluminum and titanium. The material is processed in the solution-annealed condition, known to possess anisotropic properties with pronounced hardening [1-4]. Due to difficulties in testing material with a thickness of 10.0 mm in biaxial loading, properties are assumed to follow the batch of alloy 718 with 2.6 mm presented by Pérez Caro et. al. [4] summarized in Figure 2 and Figure 3. The variations in the yield stresses and R-values as a function of the rolling direction validate the anisotropic properties of the material.

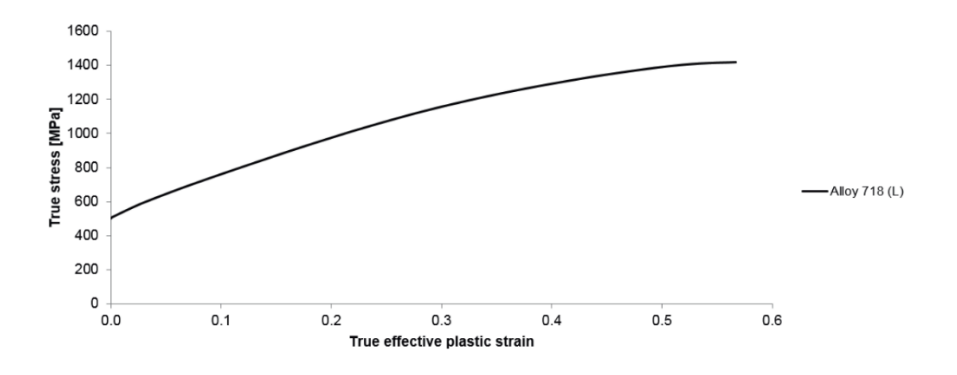


Figure 2 Flow curve for alloy 718 at room temperature.

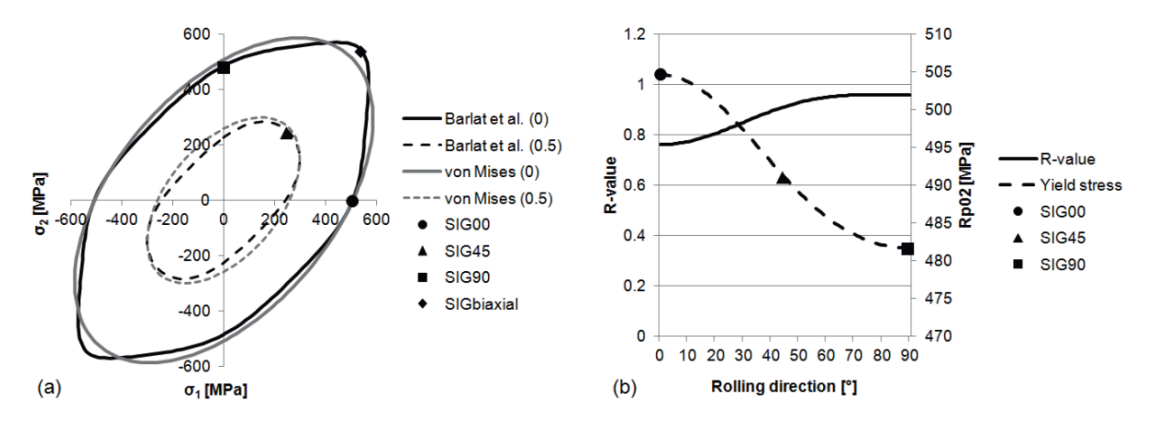


Figure 3 (a) Calibrated yield surfaces with experimental yield stresses for alloy 718 at room temperature for different values of shear stress $\sigma_{12}/\overline{\sigma}$, where σ 12 is the shear stress and $\overline{\sigma}$ is the effective stress, and (b) measured and predicted R-values and initial yield stresses depending on rolling direction at room temperature.

The material properties have been determined through performing uniaxial tensile tests with specimens extracted in three different directions with respect to the rolling direction i.e. along (00), transverse (90), and diagonal (45). From these tests, the yield stress, Lankford coefficients (R-values) and hardening was determined in these directions. Also, a viscous bulge test [4, 10] was performed producing a balanced biaxial stress state to determine the biaxial yield stress, biaxial R-value and hardening.

The Barlat Yld2000-2D [12] material model is applied in the forming simulations. The calibrated yield surface for alloy 718 along with the experimental references and anisotropy parameters are presented in Figure 3 (a) and table 1.

Table 1. Experimental yield stresses and R-values used to calibrate the yield criterion i.e. Barlat Yld2000-2D and obtaining the anisotropy parameters ($\alpha 1 - \alpha 8$).

SIG00	SIG45	SIG90	SIGbiaxial	R00	R45	R90	Rbiaxial
504.62	491.12	481.67	538.00	0.761	0.912	0.960	1.0000
α_1	α_2	Q 3	α_4	α_5	α_6	α_7	α_8
0.8711	1.1130	0.8151	0.9941	0.9875	0.8421	1.0090	1.1720

A finite element (FE) model of the Flexform process was developed. The FE model contains the tool components as well as the sheet metal blank. The blank has an element mesh consisting of 17,100 fully integrated shell elements and uses nine integration points through the plate thickness to obtain sufficient accuracy in the subsequent spring back simulation. Each element row in the radial direction of the blank covers 0.6° of the full circle. A close up of the mesh discretization before and after the forming process is displayed in Figure 4. The tool components are modeled as rigid surfaces where the friction conditions between tool surfaces and sheet metal are assumed to follow Coulomb's law. The constant friction coefficient to be used was determined based on long experience of different lubricated conditions by Quintus Technologies and by Trestad Laser. In the simulation contact between blank and rigid tool surfaces is handled by means of a surface-to-surface formulation of the mortar implementation of a forming contact [11].

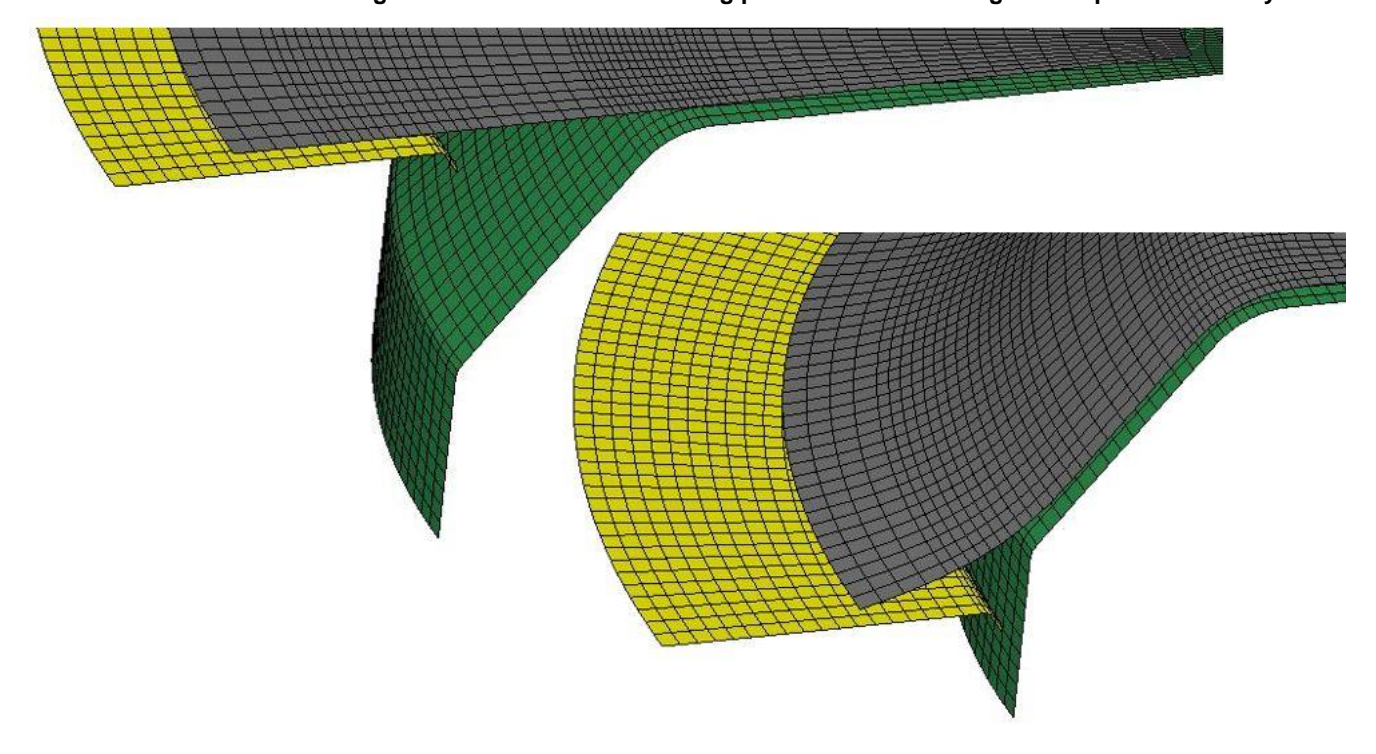


Figure 4 Mesh discretization in initial position (top image) and after completed forming (bottom image) with blank (grey), punch (green) and holder (yellow).

In the FE simulation the Flexform process is achieved by applying the pressure created by the Quintus Flexform press by means of the same technology that are used for airbag simulation during crash event simulations. For this a pressure curve as function of stroke is needed. The resulting pressure is acting on the top surface of the blank model elements. In the actual forming situation the pressure in the press acts on a thick rubber diaphragm that rests on the upside of the blank once the forming commences. The special properties of the rubber during high pressure hydrostatic loading is not taken into account in the simulations rather it is assumed that the pressure is transferred via the rubber to the blank without any influence on how the pressure is acting on the blank. The pressure profile used can be seen in Figure 5.

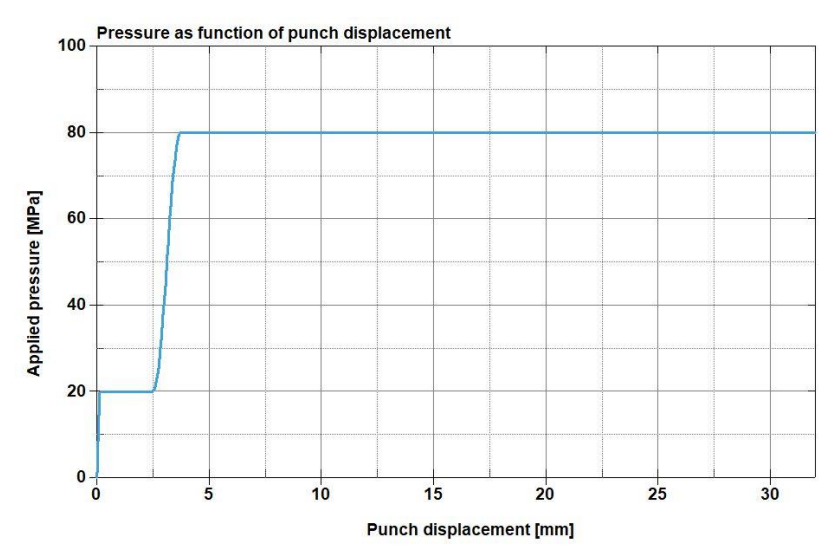


Figure 5 Applied pressure as function of punch displacement.

The anisotropic nature of the material requires the element directions to be aligned with the assumed rolling direction despite the fact that the tool and process is axisymmetric with respect to the forming direction. Depending on surface conditions and lubrication the friction between blank and the different tooling surfaces can be different which is accounted for in the model as shown in the quarter model

in Figure 6.

The process sequence simulated is shown in Figure 7 where the forming is followed by spring back, outer and inner trimming and final spring back after the trimming operations.

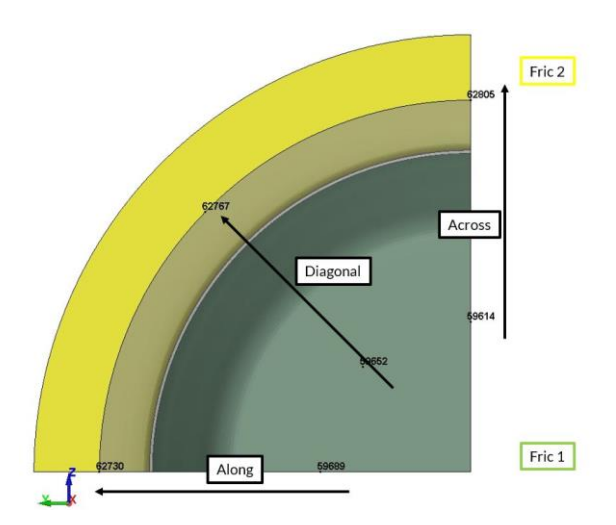


Figure 6 Quarter model in top view (viewed in forming direction) showing the different tool areas that has individual friction coefficients.

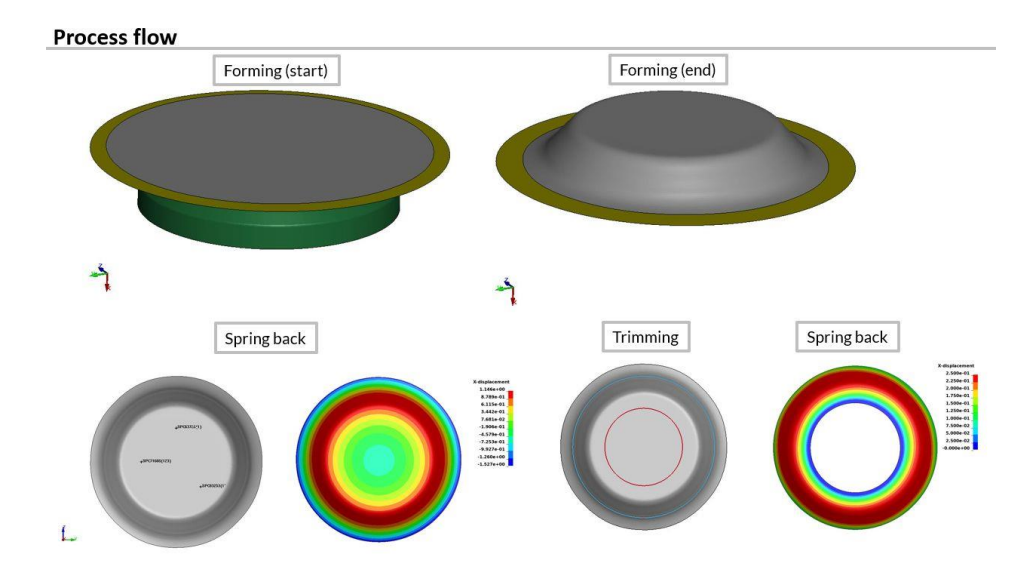


Figure 7 Illustration of the FE simulated process flow for a blank without inner hole.

3. Design and process development, Parameter studies

To enable the final part to be produced within tolerances the required product targets for the forming process were determined and analyzed by screening the influences of considered important factors [2].

For this, parameter studies using the software LS-Opt was undertaken to study the influence of sheet blank design, material properties and friction conditions on sheet thinning and spring back. The starting values are chosen to lie in the middle of the respective parameter's range so that the results should be easy to evaluate.

The variables specified are the coefficients of friction (Fric1 and Fric2) described above in Figure 6Error! Reference source not found., the yield strength of the material (Sig00) and the thickness of the initial blank (Thk). The chosen responses are sheet thinning (Thinning), thickness reduction (ThickReduction1), effective plastic strain (EFFPS) as well as calculated responses corresponding to the angular change during spring back (Ydelta (in rolling direction), YZdelta (in diagonal direction with

respect to rolling direction) and Zdelta (transverse rolling direction) illustrated above in Figure 6. Since spring back are studied, the thickness reduction relative to the original thickness need to be calculated because evaluating thickness reduction occurring during the spring back in itself is not interesting as it becomes largely insignificant. Subsequent parameter studies with different inner and outer blank diameters were undertaken. In the parameter studies only a quarter model of the part as shown in Figure 6 was used to save computational resources. The symmetry conditions used in the set-up shown in Figure 8 where nodes along the red line have constrained z-displacement and x and y rotations and nodes along the blue line have constrained y-displacement and x and z rotations.

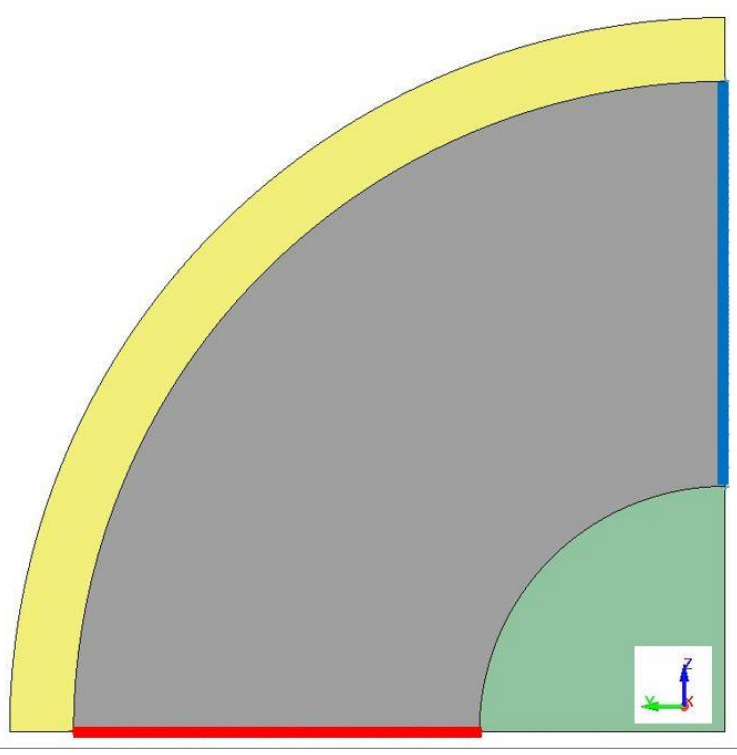


Figure 8 Boundary conditions for quarter model used in parameter studies; red line is the location for the symmetry conditions in the xy-plane and the blue line corresponding conditions in the xz-plane according to displayed coordinate triad.

For the parameter studies design of experiments using full-factor sampling of the parameter intervals has been implemented with three points per variable, which for four parameters gives 3⁴=81 data points to evaluate. Such sampling makes it possible to analyze linear relationships with variable interaction, i.e. how two factors simultaneously affect the response. There are other ways to reduce the number of simulations through stratified sampling with e.g. Latin-Hypercube or D-Optimal sampling, however here full factorial sampling was applied.

In Figure 9 the result from one parameter study with the blank without centre hole in the form of a correlation matrix is shown. In this it can be deduced that the yield stress of the material (Sig00) has the greatest influence on the spring back of the included variables (value 0.89 for all three directions). Effective plastic strain (EFFPS) and thickness reduction (ThickReduction1) are also affected by the yield stress parameter. Then follows the friction for Fric2, which has a weaker influence than the yield stress (0.22–0.23), while Fric1 has no significance for the spring back according to this analysis. The thickness of the starting material (THK) has no significance for the spring back in this study, on the other hand, the plastic strain is affected by this so that the strain decreases the thicker the starting material is (negative coefficient).

				Variables						Response		
		FRIC ¹	FRICZ	SIGO	O THK	Thin	ning Thick	Reduction EFFPS	ydelt	a vZde	zdelta Zdelta	
	FRIC1		-0.00	-0.00	-0.00	-0.03	0.24	-0.07	0.02	0.02	0.02	
bles	FRIC2			-0.00	-0.00	-0.10	0.79	-0.02	0.22	0.23	0.22	
Variables	SIG00		S 588 S		-0.00	0.05	-0.38	-0.87	0.89	0.88	0.89	
	THK					0.99	-0.08	-0.34	0.03	0.02	0.03	
_	Thinning				1	4 4	-0.20	-0.38	0.04	0.03	0.04	
020	ThickReduction1		i			111		0.36	-0.10	-0.11	-0.10	
nses	EFFPS		i	1		2 3 4	3.4	Ш.	-0.83	-0.81	-0.83	
Responses	Ydelta			ı			Frank.		الملكي	0.98	1.00	
	YZdelta									ويقاور	0.98	
	Zdelta			i						Ship on the said	معل اور	

Figure 9 Result from parameter study, blank without centre hole.

If, on the other hand a corresponding parameter study is undertaken using a blank with centre hole that additionally serves to position the blank with respect to the punch a slightly different result as can be seen in Figure 10. Here the influence from Fric 1 which is the friction between punch and blank, becomes more pronounced for the spring back behaviour as all three responses with respect to spring back increases. Still the yield stress is the dominant parameter for influencing the spring back as well as the other responses.

						Variab	Variables				Response		
		FRIC	FRIC	2 SIGO	THK	Thinn	ing Thick	Reduction 1	s ydelli	a vZde	ita Zdelta		
	FRIC1		-0.00	-0.00	-0.00	0.00	-0.04	0.02	0.42	0.41	0.42		
Variables	FRIC2			-0.00	-0.00	-0.05	0.74	-0.14	0.16	0.16	0.16		
Varia	SIG00	37 68	25 6		-0.00	0.04	-0.48	-0.87	0.76	0.76	0.76		
	THK					1.00	-0.02	-0.27	0.10	0.11	0.10		
	Thinning				3		-0.10	-0.29	0.13	0.13	0.13		
Responses	ThickReduction1		i i			1 1 1	بالكر	0.35	-0.37	-0.38	-0.37		
	EFFPS		i	i				Lie.	-0.65	-0.66	-0.65		
	Ydelta			!		A. A.		1333	-,1	1.00	1.00		
	YZdelta			!		A CANA		***			1.00		
	Zdelta					Alexander		This w		1			

Figure 10 Result from parameter study, blank with centre hole.

Figure 11 show sensitivity plots for a blank with centre hole. This comes from a linear analysis of variance (Anova). The blue bars indicate the contribution of each variable and their respective interactions to the outcome of the current response, here the spring back in the rolling direction (YDelta). In the same way as above, positive sign indicates that increasing variable values gives increasing response values and vice versa. The red thin bars show 95% confidence intervals based on the simulated substrate. The yield stress of the material has the greatest importance, followed by Fric1, which is in contrast with the case with blank without centre hole shown above in Figure 9. The third largest contribution comes from the interaction between the friction coefficients, although FRIC2 has no effect with respect to this response variable. With this screening, irrelevant variables can be sorted out for in-depth analyses of the variables that have the greatest importance.

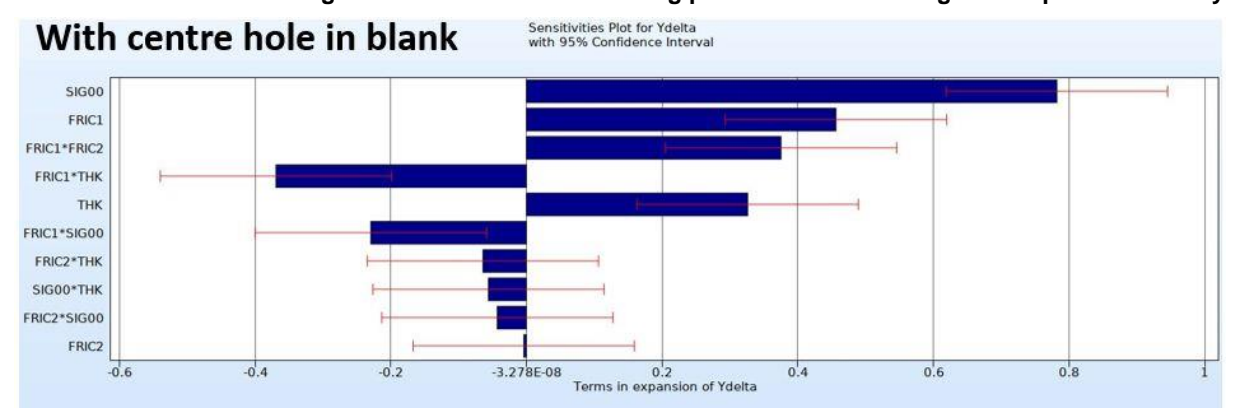


Figure 11 Sensitivity plot from the parameter study with centre hole in the blank.

The results show a small influence of the anisotropy of the material on the shape deviation of the part, which can be seen from the fact that the coefficients for the three responses that are associated with spring back are almost identical in each parameter study. Some difference, approximately 0.3 mm, in spring back occurs depending on whether the blank has a centre hole or not. Effects of anisotropy after spring back is shown in Figure 12 with YZ displacements in mm.

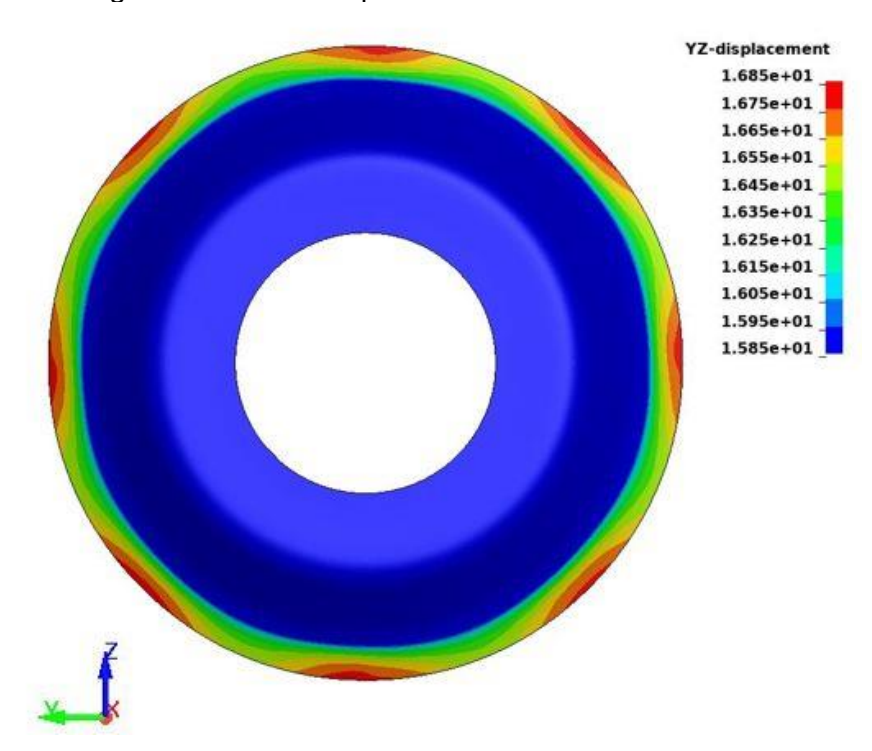


Figure 12 YZ displacement in mm after final spring back where the anisotropic effect on the flange becomes visible.

From analysis of the worst and best outcome of the parameter studies in terms of the geometric deviation from spring back, see Figure 13 the amount of compensation to be undertaken in the tooling to accomplish the most robust outcome of the forming was chosen. In addition, it was necessary to ensure that the part had sufficient thickness in the critical areas for the subsequent machining. In Figure 14 the thickness deviation with respect to the initial blank size is displayed both as a graph of the middle cross section and as a color plot. By adjusting the angle between the flat part and the conical area of the cross section without taking any anisotropy effects into account an updated punch geometry was achieved that slightly over crowns the part shape during forming. For this it was necessary to consider the margin to final part shape to allow for final machining of the part. Since the FE simulation is done using shell elements it is necessary to convert the result to a solid element part with the actual shell thickness, Figure 15 shows this conversion. The result when comparing the formed geometry to the final part shape can be seen in Figure 17. With the compensated punch geometry subsequent simulations was undertaken to determine the suitable blank geometry in terms of inner and outer radii. This enabled final manufacture of the part within tolerances after heat treatment and machining.

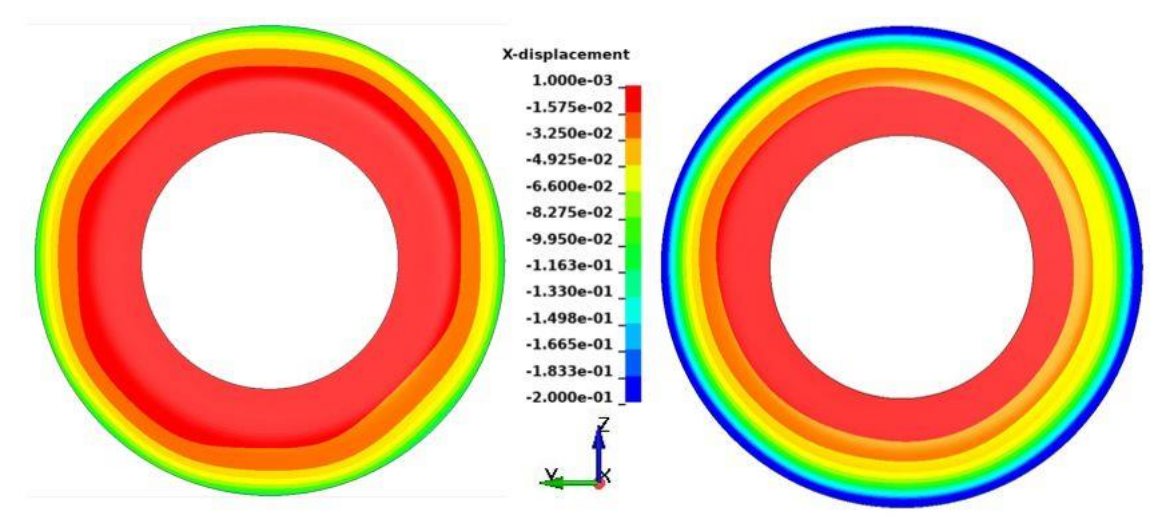


Figure 13 The spring back for parameter combinations causing minimum (left) and maximum (right) amount of spring back, NB x-axis is aligned with viewing direction i.e., into the image.

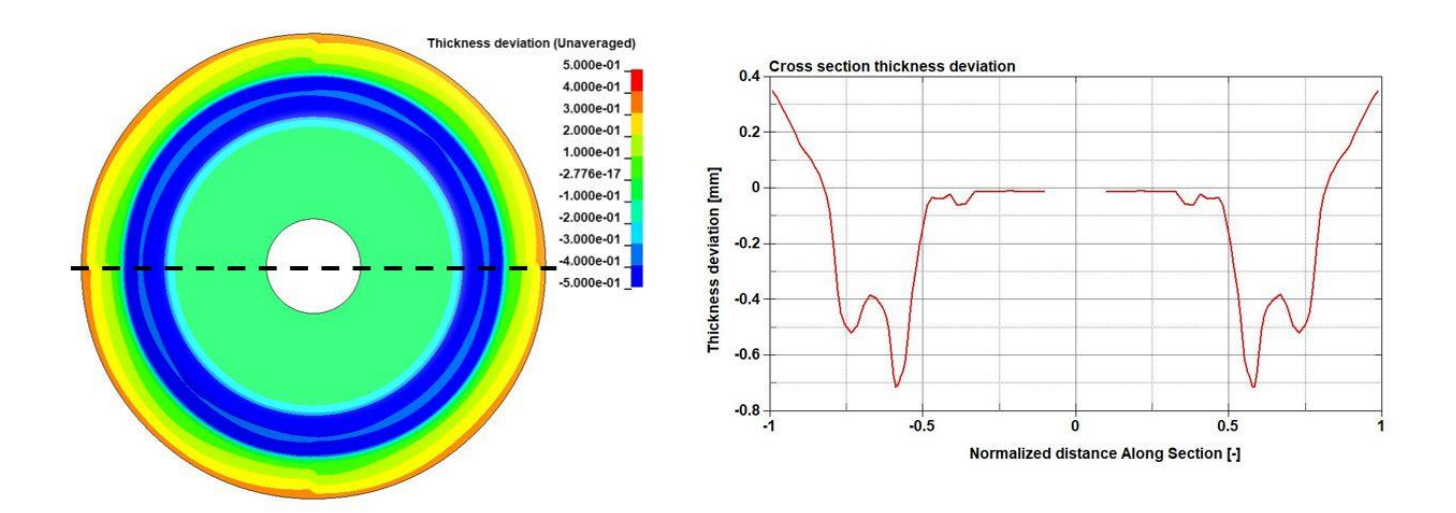


Figure 14 The resulting thickness deviation of the formed part (mm) illustrating the margin for final machining of the part, to the right the graph is showing the thickness deviation in the cross section indicated by the dashed line shown in the image to the left.

4. Full scale Process validation

In this project a flat metal sheet is Flexformed by deep drawing on a single movable Flexform tool half, designed to compensate for the simulated and expected material spring back. A central hole and the outer diameter of the blank are set to be suitable for the forming process according to the simulation studies. The central hole also provides a blank guiding feature.

To determine the possibilities for manufacturability from the simulation using shell elements a conversion from shell to solid elements using the resulting thickness obtained with the shell elements is undertaken, see Figure 15. Pictures from the actual Flexform tests are presented in Figure 16.

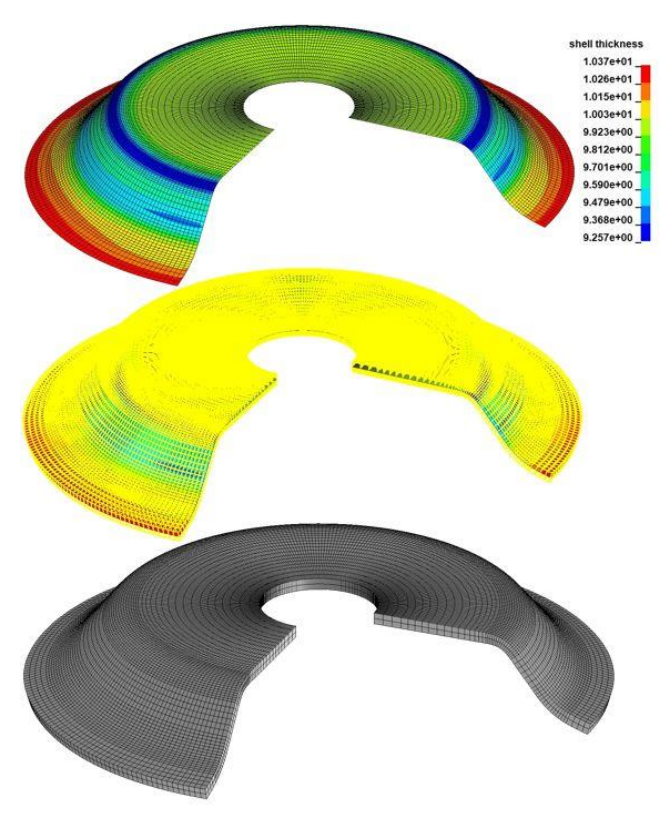


Figure 15 Expansion of shell elements into solid elements for evaluation of part manufacturability. Top image shows resulting shell thickness, middle image process in converting shell thickness to solid elements using LS-PrePost and part with resulting solid mesh in bottom image.



Figure 16 Pictures from the Flexform process illustrating the empty press table to the left, and the formed part in the middle and to the right.

After forming, the part was machined to final component geometry. The final part is visible within the formed part as illustrated in Figure 17. Two different metal sheet thicknesses were used for demonstration purpose. Both showed a good forming result.

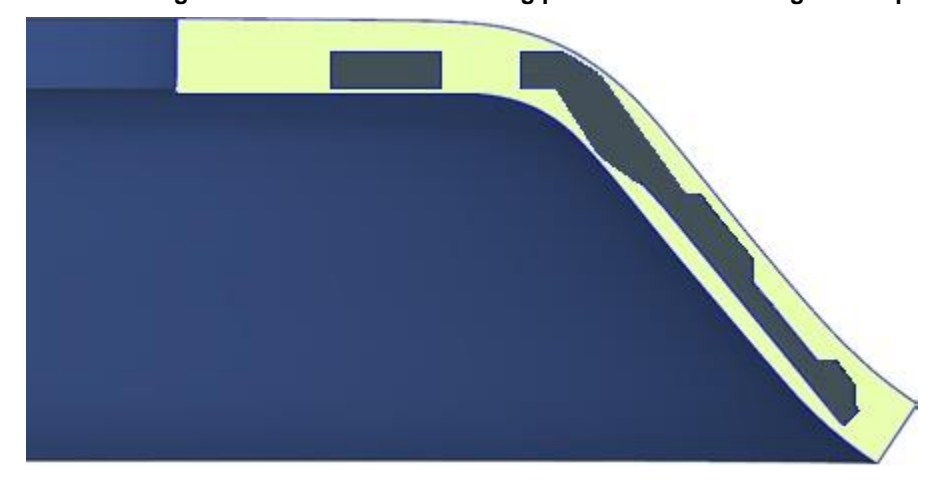


Figure 17 Illustration of the demonstrator geometry located in the formed part.

The study shows promising correlation between predicted and measured responses such as material thinning and shape deviation, see Figure 18. A 3D scanning and best fit CAD evaluation method was used to measure and evaluate the Flexformed parts and compare with the nominal CAD-geometry and spring back simulated geometry through use of STL-files exported from Ls-Dyna and the scanning and evaluation software Polyworks, Figure 19. Also, the forming tests and subsequent mechanical cutting of parts to obtain the desired geometry strongly indicates that the demonstrator part can be produced within tolerance in a highly effective way.

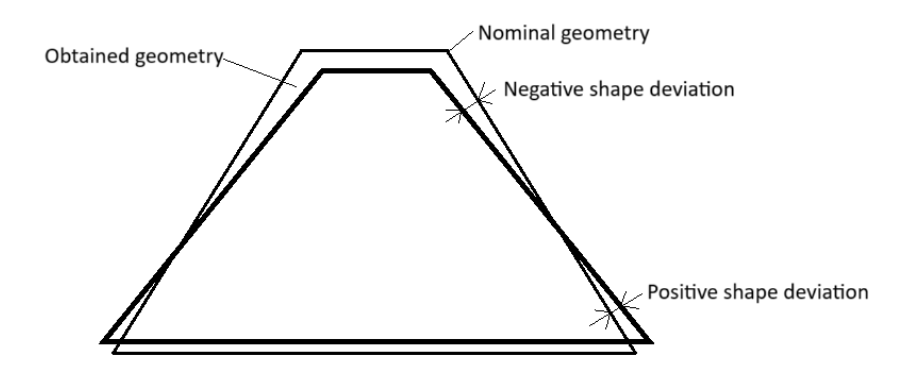


Figure 18 Illustration of the definition of shape deviation, positive and negative values applied in the study.

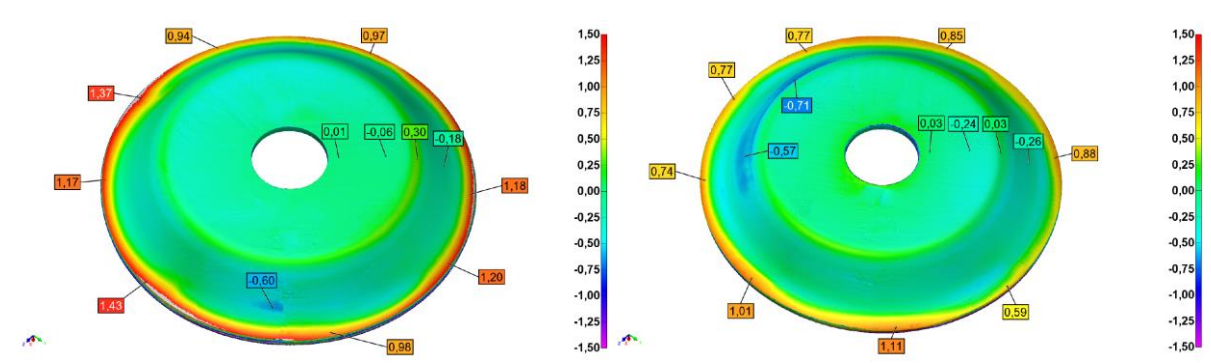


Figure 19 Illustration of predicted and measured spring back for the demonstrator geometry, respectively.

5. Summary and conclusions

In this work, a highly effective production sequence has been proposed and evaluated for the manufacturing of an aero engine component in alloy 718. The process design and parameter settings has been identified through modeling and simulation accounting for the anisotropic high strength material properties. Numerical parameter studies were performed in order to study the influence of blank design, process parameters and material properties on the predicted spring back and shape

distortion. Physical Flexform experiments were conducted to compare measured results such as material thinning and shape deviation with numerical predictions showing high correlation. Shape tolerance was predicted within 89%.

It was found that the shape tolerance of the Flexformed parts indeed could be post processed by mechanical cutting to obtain the desired demonstrator geometry within tolerances for production. Furthermore, the proposed manufacturing process chain including laser cutting of the sheet metal blank, Flexforming and mechanical cutting is considerably more effective than the existing manufacturing procedure involving more manufacturing steps and originating from forged material. GKN Aerospace Sweden has estimated energy, cost and time savings over 50% respectively. Material consumption can be reduced by at least 25%, all contributing to a substantial decrease in CO₂ emissions and environmental impact.

This study has demonstrated the potential in using the FlexformTM technology contributing to increased sustainability. Future work may be directed towards identifying other geometries of interest to the aero engine industry that would be suitable for production by the Flexform technique. In specific, parts with high shape and material thinning tolerances and advanced superalloys would be of interest. The suitable process design for each part geometry could be analyzed and optimized using FE-analysis. The project consortium intends to continue the collaboration in this area to propose new, more sustainable manufacturing methods by the involved SMEs.

6. Ackowledgements

The project funding by Vinnova grant no. 2022-01260, and the collaboration with GKN Aerospace Engine Systems Sweden AB, Quintus Technologies AB, SpeedTool AB, Trestad Laser AB and LaserTool AB are gratefully acknowledged.

7. References

- [1] Special Metals Corporation (2007) High performance alloys literature INCONEL® Alloy 718. Special Metals Corporation SMC-045. https://www.specialmetals.com/tech-center.
- [2] Odenberger, E-L., Jansson, M., Thilderkvist, P., Gustavsson, H. & Oldenburg M., A short lead time methodology for design, compensation and manufacturing of deep drawing tools for Inconel 718, *Conference Best in Class Stamping, June 16 18, 2008, Olofström, Sweden*
- [3] Pérez Caro Ll, Modelling Aspects in Forming and Welding of Nickel-Base Superalloys, PhD Thesis, Luleå University of Technology, 2019, ISSN 1402-1544
- [4] Pérez Caro Ll, Odenberger E-L, Schill M, Steffenburg-Nordenström J, Niklasson F, Oldenburg M, Prediction of shape distortions during forming and welding of a double-curved strip geometry in alloy 718, *International Journal of Advanced Manufacturing Technology*, 2020, DOI: 10.1007/s00170-020-05118-y
- [5] Coopera D. R., Rossieb K. E., Gutowsk T. G., The energy requirements and environmental impacts of sheet metalforming: An analysis of five forming processes, Journal of Materials Processing Technology, 244, pp116–135, (2017)
- [6] Palaniswamy H., Ngaile G., Altan T, Optimization of blank dimensions to reduce springback in the flexforming process, Journal of Materials Processing Technology, 146, pp 28-34 (2004)
- [7] Karaağaç I, The Evaluation of Process Parameters on Springback in V-bending Using the Flexforming Process, Materials Research, pp 1291-1299, 20(5), 2017, doi.org/10.1590/1980-5373-MR-2016-0799
- [8] Mohamed M, Carty D, Storr J, Zuelli N, Blackwell P, Savings D (2016) Feasibility Study of Complex Sheet Hydroforming Process: Experimental and Modelling, Key Engineering Materials 716:685-691.
- [9] Keshri S, Suriyanarayanan S, Analysis and Optimization of Sheet Metal Forming Processes, Chapter Hydroforming State-of-the-Art Developments and Future Trends, 1st Edition (2024) ISBN 9781003441755
- [10] Sigvant M, Mattiasson K, Vegter H, Thilderkvist P (2009) A viscous pressure bulge test for the determination of a plastic hardening curve and equibiaxial material data. Int J Mater Form 2:235-242. https://doi.org/10.1007/s12289-009-0407-y

[11] Mortar ContactAlgorithm for Implicit Stamping Analyses in LS-DYNA, T. Borrvall, 10th International LS-DYNA Users Conference 2008, Dearborn, Michigan USA

[12] Barlat F, Brem JC, Yoon JW, Chung K, Dick RE, Lege DJ, Pourboghrat F, Choi SH, Chu E (2003) Plane stress yield function for aluminium alloy sheets – part 1: theory. Int J Plast 19:1297-1319. https://doi.org/10.1016/S0749-6419(02)00019-0

Copyright Statement

The authors confirm that they, and/or their company or organization, hold copyright on all of the original material included in this paper. The authors also confirm that they have obtained permission, from the copyright holder of any third party material included in this paper, to publish it as part of their paper. The authors confirm that they give permission, or have obtained permission from the copyright holder of this paper, for the publication and distribution of this paper as part of the ICAS proceedings or as individual off-prints from the proceedings.